

Subsolidus behavior of niobian rutile from Věžná, Czech Republic: a model for exsolutions in phases with $\text{Fe}^{2+} >> \text{Fe}^{3+}$



Chování niobového rutilu z Věžné, Česká republika:
model pro odmíšení fází s $\text{Fe}^{2+} >> \text{Fe}^{3+}$ (Czech summary)

(7 text-figs, 6 tabs)

PETR ČERNÝ¹ – MILAN NOVÁK² – RON CHAPMAN¹ – MORGAN MASAU¹

¹ Department of Geological Sciences, University of Manitoba, Winnipeg, MB, Canada, R3T 2N2

² Department of Mineralogy, Petrology and Geochemistry, Masaryk University, Kotlářská 2, 611 37 Brno, Czech Republic

Niobian rutile crystallized in the Věžná I pegmatite in three generations: niobian rutile I associated with beryllian cordierite, beryl, zircon, xenotime-(Y) and monazite-(Ce), transitional into niobian rutile II in close vicinity of small pollucite-, lepidolite- and elbaite-bearing pods, and niobian rutile III in fissures with ferrocolumbite III, niobian titanite and pyrochlore-microlite. Exsolution of the niobian rutile I and II into depleted rutile and titanian ferrocolumbite is extensive. Exsolution possibly proceeded in several, presumably temperature-controlled stages. Relics of primary homogeneous niobian rutile are preserved in most crystals of generation I, but some of them and those of generation II, all perceptibly enriched in Mn, are completely exsolved. Oxide minerals of the last generation III could have been mobilized and redeposited from compositionally similar, Mn-enriched, porous aggregates of intergrowths I and II. The primary homogeneous rutile phase corresponds to rutile with 34 to 38 mol. % of ferrocolumbite component and a negligible proportion of $\text{Fe}^{3+}(\text{Nb},\text{Ta})\text{O}_4$. The depleted rutile phase shows as little as 16 mol. % ferrocolumbite, whereas the TiO_2 content of the exsolved titanian ferrocolumbite may drop to values as low as 5 mol. %. Heterovalent substitutions in niobian rutile are accomplished by $(\text{Fe},\text{Mn},\text{Mg})^{2+}_{+1}(\text{Nb},\text{Ta})^{5+}_{-2}\text{Ti}^{4+}_{-3}$, $\text{Fe}^{3+}_{+1}(\text{Nb},\text{Ta})^{5+}_{-2}\text{Ti}^{4+}_{-2}$, $\text{Sc}^{3+}_{+1}(\text{Nb},\text{Ta})^{4+}_{-1}\text{Ti}^{4+}_{-2}$, and $(\text{Fe},\text{Mn},\text{Mg})^{2+}_{+1}\text{W}^{6+}_{-1}\text{Ti}^{4+}_{-2}$. With negligible and undecipherable additional substitutions, reverse mechanisms control ferrocolumbite: $(\text{Fe},\text{Sc})^{3+}_{+3}(\text{Nb},\text{Ta})^{5+}_{-2}(\text{Fe},\text{Mn},\text{Mg},\text{Ca})^{2+}_{-1}$, $(\text{Nb},\text{Ta})^{5+}_{-4}$, and $(\text{Ti},\text{Zr},\text{Hf})^{4+}_{+3}(\text{Fe},\text{Mn},\text{Mg},\text{Ca})^{2+}_{-1}(\text{Nb},\text{Ta})^{5+}_{-2}$. Exsolution concentrates Mg, Mn, Fe^{2+} , Fe^{3+} , Sc, Zr, Hf, U, Nb, Ta and W in the exsolved ferrocolumbite. In relative terms, rutile conserves Sn, Fe^{2+} , Fe^{3+} , Ta, and Fe^{3+} relative to Fe^{2+} , whereas Mn and Nb are preferred by the columbite structure. The ZrO_2 content of primary homogeneous niobian rutile is ≤ 0.34 wt. % but the exsolved ferrocolumbite contains as much as 2.11 wt. % along with ≤ 0.16 wt. % HfO_2 . These concentrations confirm that Zr and Hf must be considered significant minor elements in niobian rutile from granitic environments. Considerable enrichment in Mg, ≤ 0.34 wt. % MgO in primary homogeneous niobian rutile and ≤ 2.16 wt. % MgO in exsolved ferrocolumbite, can be presumed a local feature, reflecting contamination of the pegmatite by serpentinite wallrock.

Key words: rutile, ferrocolumbite, niobium, tantalum, zirconium, hafnium, order-disorder, exsolution, granitic pegmatite, Czech Republic.

Introduction

Niobian rutile (a. k. a. ilmenorutile) from Věžná, south of Rožná near Bystřice nad Pernštejnem in western Moravia, was first examined by Černý – Čech (1962). The results of a more thorough investigation of this mineral were published by Černý et al. (1964). Optical and X-ray powder diffraction studies revealed heterogeneous phase composition, but wet chemical analyses could provide only bulk compositions of a few specimens restricted to the major components, and a single composition of a pure rutile phase. Here we report on the electron-microprobe and X-ray powder diffraction studies of the Věžná niobian rutile, in part based on samples used by previous investigators, the results of which are shedding a new light on this “old” mineral. We also provide data on two late generations of this phase, discovered since the publication of the papers quoted above.

The parent pegmatite and mineral assemblage

The Věžná I pegmatite which yielded abundant niobian rutile is situated in a tectonic slab of serpentinite, enclosed in migmatitic gneiss about 1 km south of the village of Věžná. According to Černý – Novák (1992), the pegmatite consists of a narrow, intermittent coarse-

grained granitic wall zone of K-feldspar + oligoclase + quartz + biotite, a dominant intermediate zone of graphic K-feldspar (>oligoclase) + quartz, with local graphic aggregates of cleavelandite + quartz, grading into an intermediate zone (core-margin) of blocky K-feldspar + subordinate cleavelandite, which surrounds isolated central pods of a quartz core. An asymmetric, intermittent unit of albite-oligoclase, imbedded in a phlogopite (+ apatite, tourmaline) matrix (Černý – Miškovský 1966), follows the footwall contact. Reaction rim of anthophyllite, actinolite and phlogopite is developed along the pegmatite contacts with the host serpentinite. Beryllian cordierite (Černý – Povondra 1966), niobian rutile I, ferrocolumbite, monazite-(Ce), xenotime-(Y), zircon, beryl and schorl to dravite constitute the main assemblage of accessory minerals.

Rare small pods of brownish K-feldspar + quartz carry lepidolite (in part Cs-dominant), elbaite, beryl, tripelite, apatite, brabantite, huebnerite, Ta-enriched niobian rutile II, hafnan zircon, bismuth, pollucite, analcime, harmotome and chabasite (Novák – Pelz 1981, Teertstra et al. 1995). These pods represent the maximally fractionated tail-end of primary crystallization, plus a hydrothermal end-stage, of the pegmatite consolidation.

Low-temperature hydrothermal association of breakdown products includes milarite (Černý 1960, Černý

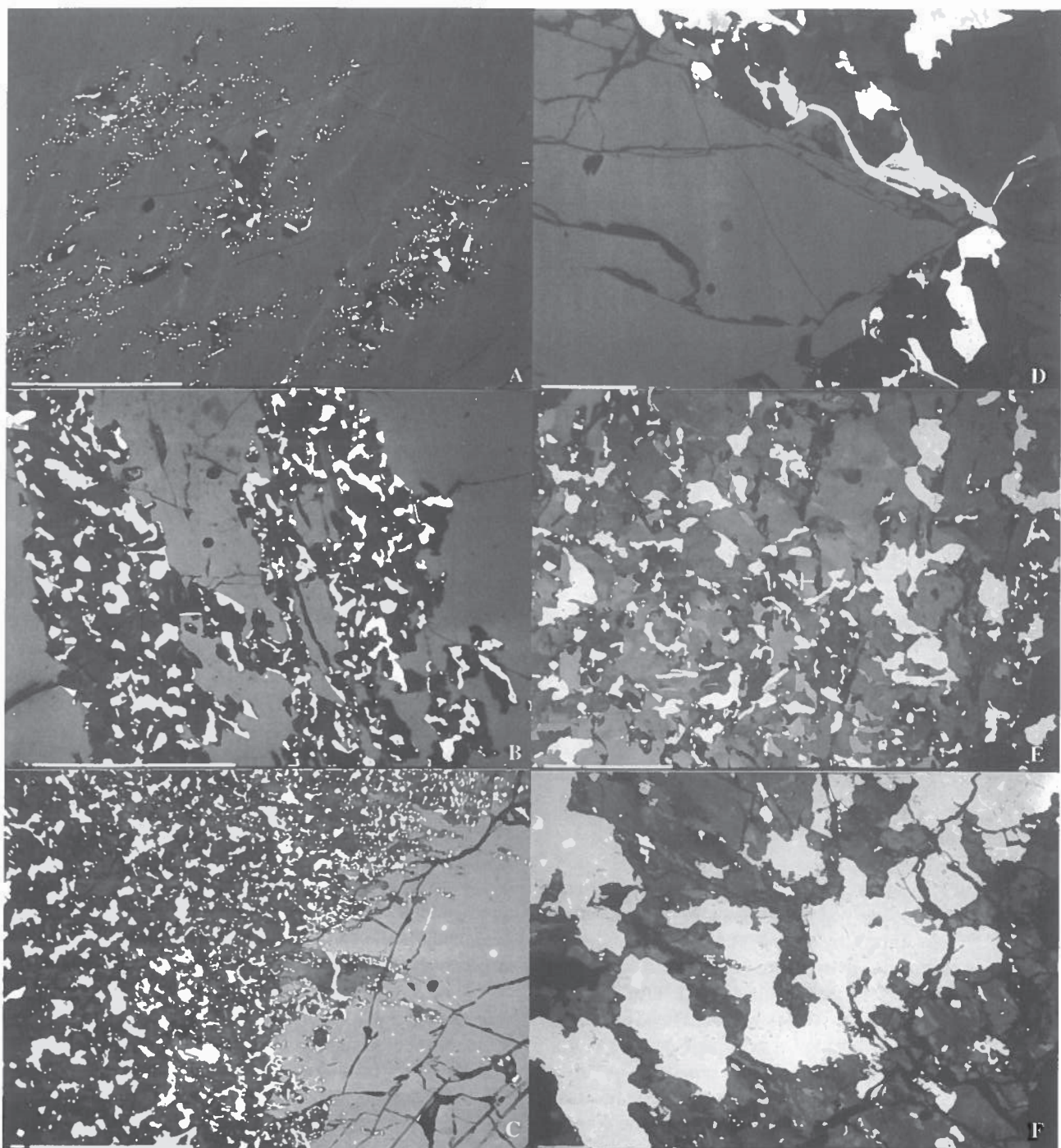


Fig. 1. Backscattered-electron images of the Věžná I niobian rutile I in various stages of exsolution: A – primary homogeneous niobian rutile (medium-grey matrix) with diffuse Fe, Nb, Ta-enriched streaks (pale-grey) and local clusters of depleted rutile (near-black) with exsolved ferrocolumbite (white) (scale bar 200 µm) (see Table 2 for compositions of all phases); B – belts of very fine-grained early-stage exsolution of ferrocolumbite (white) from depleted niobian rutile (black) in the matrix of primary homogeneous niobian rutile (dark grey) (scale bar 200 µm); C – progressive coarsening and increasing degree of exsolution in the intergrowth of depleted niobian rutile (dark grey to black) + ferrocolumbite (white) from the primary homogeneous niobian rutile (pale-grey at bottom right) outwards (scale bar 500 µm); D – very coarse-grained intergrowth of depleted niobian rutile (dark-grey) + ferrocolumbite (white) developing directly from the adjacent primary homogeneous niobian rutile (medium-grey) (scale bar 200 µm); E – exsolution intergrowth of depleted niobian rutile (mottled grey) and ferrocolumbite (white), typical of most of the niobian rutile I, with compositions of rutile variable over the three maxima shown in Fig. 5 and represented in Table 3 (scale bar 200 µm); F – the coarsest-grained exsolution intergrowth of depleted niobian rutile (variable grey) + more or less manganese-rich ferrocolumbite (white) with most extreme compositions of both phases, close to those represented in Table 4 and Fig. 3C, F (scale bar 200 µm).

et al. 1980, Hawthorne et al. 1991) bavenite, eudidymite, epididymite, celadonite (Černý 1968), bertrandite (Novák et al. 1991) and microlite (Čech 1963). These minerals are mainly found in thin fissures crosscutting the early rock-forming and accessory phases. Discrete crystals of niobian rutile III and associated titanian ferrocolumbite III belong to this general category of late hydrothermal phases; they reside on quartz lining the fissures in feldspar and quartz, associated with a Pb-rich pyrochlore-microlite phase and titanite containing up to 11 wt. % Nb_2O_5 and 4 wt. % Ta_2O_5 .

Experimental

Electron-microprobe analyses of the niobian rutile and titanian ferrocolumbite were performed in the wavelength-dispersion mode on a Cameca SX-50 instrument at the Department of Geological Sciences, University of Manitoba. A beam diameter of 1 to 2 μm , accelerating potential of 15 kV, a sample current of 20 mA and a counting time of 20 s were used for Ti, Nb, Ta, Fe and Mn, and 40 mA and 50 s for W, Sb, Bi, As, Sc, Ca, Pb, Y, U, Zr and Hf. The following standards were used: manganotantalite ($\text{TaM}\alpha$), MnNb_2O_6 ($\text{MnK}\alpha$, $\text{NbL}\alpha$), FeNb_2O_6 ($\text{FeK}\alpha$), CaNb_2O_6 ($\text{CaK}\alpha$), SnO_2 ($\text{SnL}\alpha$), rutile ($\text{TiK}\alpha$), BiTaO_4 ($\text{BiM}\alpha$), mimetite ($\text{PbM}\alpha$, AsLa), stibiotantalite ($\text{SbL}\alpha$), $\text{NaScSi}_2\text{O}_6$ ($\text{ScK}\alpha$), UO_2 ($\text{UM}\alpha$), YAG ($\text{YL}\alpha$), ZrO_2 ($\text{ZrL}\alpha$), metallic Hf ($\text{HfK}\alpha$) and metallic W ($\text{WM}\alpha$). Data were reduced using the PAP routine (Pouchou & Pichoir 1984, 1985).

The data for both rutile and columbite phases were normalized to 8 oxygen atoms and 4 cations for easy mutual comparison; this corresponds to the unit-cell content of ixiolite and disordered columbite-tantalite (Černý – Ercit 1989) and to 2 unit-cell contents of rutile. This treatment calculates the content of Fe^{3+} , a routine legitimized experimentally on the example of wodginite by Ercit et al. (1992). In both cases, the data correspond to atoms per 4 formula units ($\text{ap}4\text{fu}$).

It is noteworthy that the compositions established by Pavel Povondra thirty-five years ago by wet chemical analysis (Černý et al. 1964) are in good agreement with the results of electron-microprobe data, by direct comparison of the compositions of homogeneous phases and by comparing the results of bulk wet analysis with integrated data on the niobian rutile + ferrocolumbite intergrowths. The only significant difference is a systematic shift toward a slightly lower Nb/Ta ratio in the EMPA data.

Unit-cell dimensions were refined from X-ray powder diffraction data, collected on the Philips 1710 automated powder diffractometer. Annealed CaF_2 with $a = 5.46379(4)$ Å, calibrated against a NBS silicon reference (batch 640; $a = 5.430825$ Å), was used as an internal standard. Refinements were done using the FIX program for reduction of systematic error in positional data of X-ray powder diffraction maxima to $+0.01^\circ 2\theta$ (Ercit 1986), and a modified version of the CELREF least-squares program of Appleman – Evans (1973).

Table 1. Representative chemical compositions of primary homogeneous niobian rutile I from the Věžná I pegmatite (cf. Fig. 2A, E). Atomic contents based on 8 oxygen atoms and 4 cations (see "Experimental" for details).

	N40–4	N41A–4	22B–1	A73C–8	A64C–8	A74F–2
WO_3	0.85	0.59	1.03	0.72	0.65	0.50
Nb_2O_5	27.88	26.24	27.99	27.47	26.68	26.51
Ta_2O_5	6.72	8.16	6.80	6.25	6.74	6.20
TiO_2	52.80	53.54	54.06	54.62	55.48	56.18
ZrO_2	0.28	0.12	0.10	0.21	0.20	0.12
HfO_2	0.00	0.00	0.00	0.00	0.00	0.00
SnO_2	0.45	0.50	0.46	0.35	0.46	0.57
ThO_2	0.00	0.00	0.00	0.00	0.00	0.00
UO_2	0.01	0.03	0.03	0.04	0.04	0.03
Sc_2O_3	0.23	0.33	0.32	0.26	0.17	0.32
Fe_2O_3	0.67	1.24	1.08	2.44	0.84	2.41
As_2O_3	0.00	0.00	0.00	0.00	0.00	0.00
Y_2O_3	0.02	0.00	0.06	0.04	0.00	0.03
Sb_2O_3	0.00	0.00	0.04	0.00	0.00	0.00
Bi_2O_3	0.00	0.00	0.00	0.03	0.05	0.03
MgO	0.33	0.30	0.30	0.15	0.29	0.24
CaO	0.00	0.00	0.01	0.01	0.01	0.00
MnO	0.04	0.08	0.13	0.05	0.06	0.06
FeO	7.83	7.26	7.63	7.08	7.44	6.54
ZnO	0.00	0.00	0.00	0.00	0.00	0.04
PbO	0.00	0.00	0.00	0.00	0.00	0.00
TOTAL	98.12	98.38	100.04	99.72	99.11	99.78
W	0.014	0.010	0.017	0.012	0.011	0.008
Nb	0.807	0.758	0.794	0.777	0.759	0.745
Ta	0.117	0.142	0.116	0.106	0.115	0.105
Ti	2.542	2.574	2.551	2.570	2.625	2.625
Zr	0.009	0.004	0.003	0.006	0.006	0.004
Hf	0.000	0.000	0.000	0.000	0.000	0.000
Sn	0.011	0.013	0.012	0.009	0.012	0.014
Th	0.000	0.000	0.000	0.000	0.000	0.000
U	0.000	0.000	0.000	0.001	0.001	0.000
Sc	0.013	0.018	0.017	0.014	0.009	0.017
Fe^{3+}	0.032	0.059	0.051	0.115	0.040	0.113
As	0.000	0.000	0.000	0.000	0.000	0.000
Y	0.001	0.000	0.002	0.001	0.000	0.001
Sb	0.000	0.000	0.001	0.000	0.000	0.000
Bi	0.000	0.000	0.000	0.000	0.001	0.000
Mg	0.031	0.029	0.028	0.014	0.027	0.022
Ca	0.000	0.000	0.001	0.001	0.001	0.000
Mn	0.002	0.004	0.007	0.003	0.003	0.003
Fe^{2+}	0.419	0.388	0.400	0.371	0.392	0.340
Zn	0.000	0.000	0.000	0.000	0.000	0.002
Pb	0.000	0.000	0.000	0.000	0.000	0.000

Niobian rutile I and titanian ferrocolumbite I

Coarse columnar crystals of the Věžná I niobian rutile I attain maximum dimensions of 2 x 10 cm. They constitute six-sided prisms elongated parallel to the [101] direction, with pyramidal and prismatic faces in their terminations (cf. Fig. 1 in Černý – Čech 1962). Twinning on (101) is common, occasionally in a cyclic form. The crystals are locally conical and hollow, with rather smooth crystal faces on the outside but with coarsely grooved internal surface, adjoining cores of feldspar or quartz. The niobian rutile is steel-grey to black, with fracture surfaces either conchooidal and highly lustrous or finely to coarsely granular and dull. Optical examination in reflected light shows the lustrous mineral to be homo-

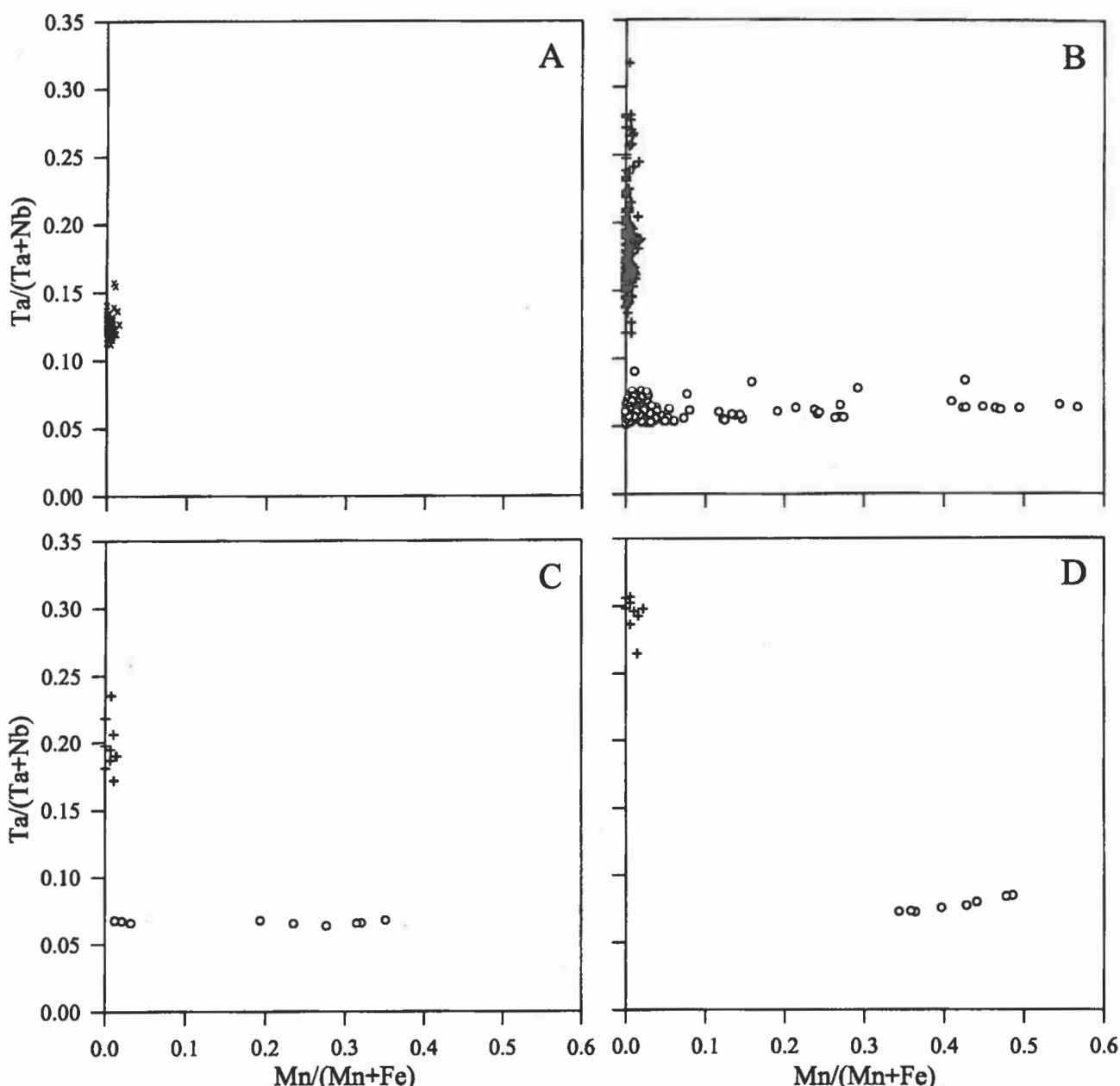


Fig. 2. Compositions of the Věžná I niobian rutile in the columbite quadrilateral (A to D) and in the ternary diagram ($\text{Nb}+\text{Ta}$) – ($\text{Ti}+\text{Sn}+\text{Zr}+\text{Hf}$) – ($\text{Fe}_{\text{tot}}+\text{Mn}+\text{Mg}+\text{Sc}$) (E to H), both in atomic proportions. A and E – primary homogeneous rutile I (cf. Table 1); B and F – depleted rutile I and exsolved titanian columbite (cf. Tables 2 to 4); C and G – niobian rutile II from near Li, Cs-enriched pods (cf. Table 5); D and H – discrete crystals of niobian rutile III and associated titanian columbite from open fissures (cf. Table 6). X – primary niobian rutile, + – depleted niobian rutile, o – exsolved titanian ferrocolumbite.

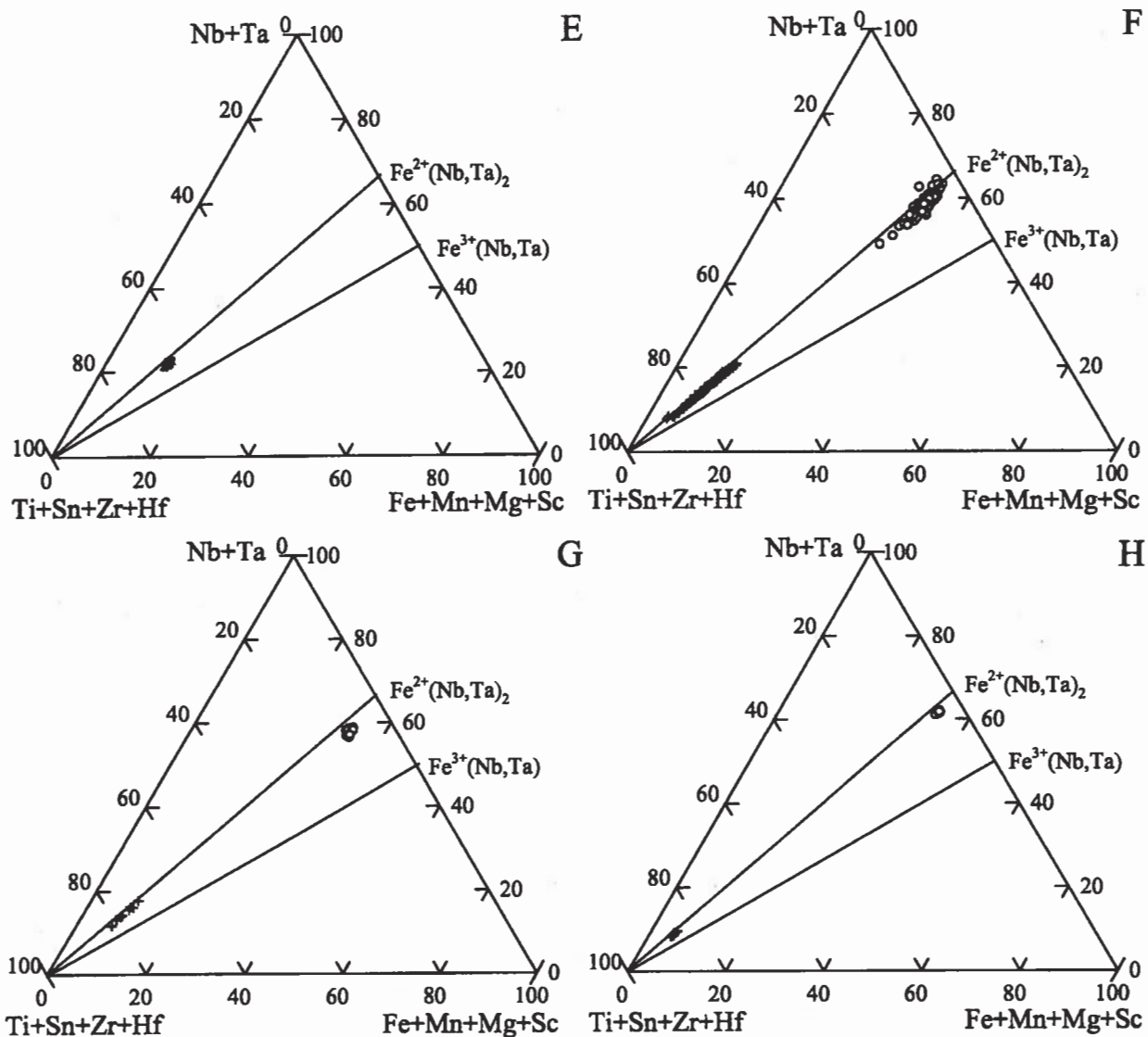
geneous, whereas the granular material shows numerous microscopic grains of a darker titanian ferrocolumbite, verified by X-ray powder diffraction. Coarse-granular intergrowths are occasionally slightly porous.

The homogeneous niobian rutile I represents relics of the primary phase, which yielded depleted niobian rutile and ferrocolumbite upon exsolution (Černý – Čech 1962, Čech et al. 1964, Černý et al. 1964). The exsolution is rarely observed to start as diffuse Nb, Ta-enriched streaks in rutile, 30 to 150 µm long and 3 to 10 µm wide, possibly still with a rutile structure suggested by their gradual transition into the primary rutile matrix (Fig. 1A). In most cases the exsolution initially produces very fine-

grained ferrocolumbite (3 to 20 µm) in depleted niobian rutile matrix (Fig. 1A, B), with gradual coarsening of both phases (Fig. 1C). Occasionally, however, the texturally and compositionally defined first products of exsolution are quite coarse-grained (Fig. 1D). Granular ferrocolumbite (20 to 150 µm) in heterogeneous rutile matrix is the most abundant type of intergrowth in the niobian rutile I (Fig. 1E). Extreme coarsening of the exsolution intergrowth generates grains of more or less manganan ferrocolumbite up to 1 mm, rarely 3 mm in size (Fig. 1F).

Composition of the primary homogeneous phase I is quite uniform, and it corresponds to rutile with 38 to

Fig. 2 (continued)



34 mol. % of the $(\text{Fe} > \text{Mn})(\text{Nb} > \text{Ta})_2\text{O}_6$ (ferrocolumbite) component. The content of the $\text{Fe}^{3+}(\text{Nb} > \text{Ta})\text{O}_4$ component (so far unknown as an independent mineral species) is negligible (Table 1, Fig. 2A, E). The diffuse streaks indicative of the incipient exsolution are only very slightly enriched in Nb, Ta, Sc, Fe^{3+} and Mn relative to the surrounding matrix (Table 2). In contrast, the compositions of depleted niobian rutile I and exsolved ferrocolumbite I (R and FC in Table 2; Figs 2B, F, 3A, B) are distinctly different from those of the early-stage products, and the difference increases with continuing exsolution and recrystallization (Tables 3 and 4; Figs 2B, F, 3C, D and E, F). With progressive exsolution, Mg, Mn, Fe^{2+} , Fe^{3+} , Sc, Zr, Hf, U, Nb, Ta and W become concentrated in the ferrocolumbite phase; in relative terms, rutile conserves Sn, Fe^{3+} and Ta, and Fe^{3+} relative to Fe^{2+} , whereas Mn, Mg and Nb are preferred by the columbite structure (Figs 2, 3). This is reflected, for example, by changes in the $\text{Fe}^{2+}/(\text{Fe}^{2+}+\text{Fe}^{3+})$ and $\text{Fe}^{2+}/(\text{Fe}^{2+}+\text{Mg})$ ratios (Fig. 4).

Statistics of the Ti content of depleted rutile I suggest a trimodal distribution, whereas the histogram of Ti in ferrocolumbite I is more compact and polymodal distribution is far from obvious (Fig. 5).

A small proportion of exsolved titanian ferrocolumbite I is distinctly enriched in Mn, with $\text{Mn}/(\text{Mn}+\text{Fe})$ between 0.18 and 0.57 and with two compositions corresponding to ferroan manganocolumbite (cf. Table 4 and Figs 2B, F, 3E, F). This enrichment in Mn is typical of samples which show maximum depletion of, and some of the highest $\text{Ta}/(\text{Ta}+\text{Nb})$ values in the rutile matrix, and which do not contain relics of primary homogeneous niobian rutile.

The content of Hf in the primary homogeneous rutile is below the detection limits of the experimental conditions employed, but ZrO_2 attains up to 0.34 wt. %. The exsolved ferrocolumbite shows $\text{ZrO}_2 \leq 2.06$ wt. % and $\text{HfO}_2 \leq 0.16$ wt. %. The maximum content of 2.16 wt. % MgO in ferrocolumbite also is remarkable, equal to

Table 2. Representative chemical compositions of primary homogeneous niobian rutile I from the Věžná I pegmatite and its incipient breakdown products: RP – primary niobian rutile, D – diffuse streaks of Nb, Ta-enriched (rutile?) phase, R – depleted niobian rutile, FC – exsolved titanian ferrocolumbite. Atomic contents based on 8 oxygens atoms and 4 cations (see “Experimental” for details). The data were collected from the area shown in Fig. 1A.

	A64D-3 RP	A64D-10 RP	A64D-4 D	A64D-9 D	A64D-6 R	A64D-1 FC
WO ₃	0.67	0.62	0.68	0.50	0.71	2.44
Nb ₂ O ₅	27.88	27.99	28.67	28.45	22.78	55.19
Ta ₂ O ₅	7.00	6.76	7.10	7.30	7.28	7.32
TiO ₂	54.69	54.93	53.45	53.41	61.10	16.17
ZrO ₂	0.29	0.29	0.23	0.28	0.07	1.26
HfO ₂	0.00	0.00	0.00	0.00	0.00	0.09
SnO ₂	0.57	0.59	0.53	0.49	0.57	0.35
ThO ₂	0.00	0.00	0.00	0.00	0.00	0.02
UO ₂	0.06	0.13	0.00	0.15	0.00	0.25
Sc ₂ O ₃	0.25	0.25	0.33	0.31	0.17	1.13
Fe ₂ O ₃	0.51	0.96	1.50	1.51	0.24	0.83
As ₂ O ₃	0.00	0.00	0.00	0.00	0.00	0.00
Y ₂ O ₃	0.00	0.02	0.03	0.01	0.00	0.05
Sb ₂ O ₃	0.06	0.05	0.03	0.01	0.00	0.05
Bi ₂ O ₃	0.00	0.03	0.00	0.00	0.05	0.07
MgO	0.28	0.31	0.32	0.32	0.22	1.90
CaO	0.01	0.00	0.00	0.01	0.00	0.00
MnO	0.04	0.05	0.07	0.10	0.06	1.01
FeO	7.95	7.67	7.61	7.49	6.90	11.45
ZnO	0.00	0.00	0.00	0.01	0.00	0.00
PbO	0.01	0.00	0.00	0.00	0.00	0.00
TOTAL	100.27	100.65	100.55	100.35	100.15	99.58
W	0.011	0.010	0.011	0.008	0.011	0.046
Nb	0.789	0.788	0.811	0.807	0.632	1.798
Ta	0.119	0.114	0.121	0.125	0.122	0.143
Ti	2.573	2.571	2.515	2.519	2.820	0.876
Zr	0.009	0.009	0.007	0.009	0.002	0.044
Hf	0.000	0.000	0.000	0.000	0.000	0.002
Sn	0.014	0.015	0.013	0.012	0.014	0.010
Th	0.000	0.000	0.000	0.000	0.000	0.000
U	0.001	0.002	0.000	0.002	0.000	0.004
Sc	0.014	0.014	0.018	0.017	0.009	0.071
Fe ₃₊	0.024	0.045	0.071	0.071	0.011	0.045
As	0.000	0.000	0.000	0.000	0.000	0.000
Y	0.000	0.001	0.001	0.000	0.000	0.002
Sb	0.002	0.001	0.001	0.000	0.000	0.001
Bi	0.000	0.000	0.000	0.000	0.001	0.001
Mg	0.026	0.029	0.030	0.030	0.020	0.204
Ca	0.001	0.000	0.000	0.001	0.000	0.000
Mn	0.002	0.003	0.004	0.005	0.003	0.062
Fe ₂₊	0.416	0.399	0.398	0.393	0.354	0.690
Zn	0.000	0.000	0.000	0.000	0.000	0.000
Pb	0.000	0.000	0.000	0.000	0.000	0.000

17 mol. % of the magnocolumbite component. The Sc content of the primary homogeneous niobian rutile is modest but it considerably increases in the exsolved ferrocolumbite I: ≤ 0.39 and ≤ 1.90 wt. % Sc₂O₃, respectively.

X-ray powder diffraction data of the rutile phase show the monorutile structure in both natural state and after heating to 1000 °C for 16 hours in air. Ferrocolumbite I has a disordered ixiolite-type structure which turns on heating into an ordered state of proper columbite (see Černý – Turnock 1971 and Ercit et al. 1995 for order/disorder relationships in the columbite group).

Table 3. Chemical compositions of intermediate-stage exsolution products of primary niobian rutile I (R) from the Věžná I pegmatite, representative of the trimodal distribution of rutile compositions illustrated Fig. 5A, and of associated ferrocolumbite I (FC). Atomic contents based on 8 oxygens atoms and 4 cations (see “Experimental” for details). Note the rapid depletion of Nb, Ta, Fe and other elements in rutile, and a modest decrease in Ti in ferrocolumbite, with the degree of exsolution increasing from the modal maximum 1 through 2 to 3.

	A73E-5 R1	A73E-3 FC1	A74D-5 R2	A74D-12 FC2	A73C-11 R3	A73C-14 FC3
WO ₃	0.12	2.33	0.33	6.17	0.09	3.59
Nb ₂ O ₅	22.62	62.13	17.01	60.36	15.18	65.15
Ta ₂ O ₅	6.42	6.85	6.36	6.23	5.99	6.41
TiO ₂	62.04	8.35	67.67	6.88	70.85	4.05
ZrO ₂	0.02	1.53	0.00	0.27	0.00	0.00
HfO ₂	0.00	0.10	0.00	0.04	0.00	0.00
SnO ₂	0.49	0.23	1.09	0.39	1.09	0.27
ThO ₂	0.00	0.00	0.04	0.01	0.04	0.00
UO ₂	0.02	0.07	0.06	0.10	0.01	0.06
Sc ₂ O ₃	0.09	1.54	0.03	1.39	0.03	0.97
Fe ₂ O ₃	1.78	0.45	1.96	0.70	2.29	0.29
As ₂ O ₃	0.00	0.00	0.01	0.00	0.00	0.00
Y ₂ O ₃	0.00	0.05	0.02	0.05	0.00	0.04
Sb ₂ O ₃	0.02	0.00	0.03	0.00	0.00	0.02
Bi ₂ O ₃	0.00	0.00	0.14	0.00	0.00	0.20
MgO	0.13	2.11	0.04	1.18	0.06	0.73
CaO	0.00	0.00	0.00	0.00	0.00	0.00
MnO	0.05	0.77	0.01	2.20	0.02	4.71
FeO	6.06	13.07	4.72	13.79	3.92	13.01
ZnO	0.00	0.00	0.00	0.07	0.00	0.00
PbO	0.00	0.00	0.00	0.00	0.04	0.00
TOTAL	99.86	99.57	99.52	99.83	99.61	99.50
W	0.002	0.045	0.005	0.121	0.001	0.071
Nb	0.624	2.075	0.463	2.058	0.407	2.249
Ta	0.106	0.138	0.104	0.128	0.097	0.133
Ti	2.845	0.464	3.064	0.390	3.163	0.233
Zr	0.001	0.055	0.000	0.010	0.000	0.000
Hf	0.000	0.002	0.000	0.001	0.000	0.000
Sn	0.012	0.007	0.026	0.012	0.026	0.008
Th	0.000	0.000	0.001	0.000	0.001	0.000
U	0.000	0.001	0.001	0.002	0.000	0.001
Sc	0.005	0.099	0.002	0.091	0.002	0.065
Fe ₃₊	0.082	0.025	0.089	0.040	0.102	0.017
As	0.000	0.000	0.000	0.000	0.000	0.000
Y	0.000	0.002	0.001	0.002	0.000	0.002
Sb	0.001	0.000	0.001	0.000	0.000	0.001
Bi	0.000	0.000	0.002	0.000	0.000	0.004
Mg	0.012	0.232	0.004	0.133	0.005	0.083
Ca	0.000	0.000	0.000	0.000	0.000	0.000
Mn	0.003	0.048	0.001	0.141	0.001	0.305
Fe ₂₊	0.309	0.807	0.237	0.870	0.195	0.830
Zn	0.000	0.000	0.000	0.004	0.000	0.000
Pb	0.000	0.000	0.000	0.000	0.001	0.000

Unit-cell dimensions of the rutile and columbite phases cannot be correlated with the compositional data, as the X-rayed powder mounts represent averages of considerably heterogeneous samples. Nevertheless, the rutile phase (a 4.636 to 4.639, c 2.984 to 2.992 Å for primary, a 4.601 to 4.620, c 2.975 to 2.983 Å for depleted) generally corresponds to niobian rutile examined by Černý et al. (1964), and the titanian ferrocolumbite yields values (a ~4.7 to 4.75, b ~5.72 to 5, 75, c ~5.12 Å) expected for disordered phases of such composition (cf. Černý – Ercit 1989, Ercit et al. 1995).

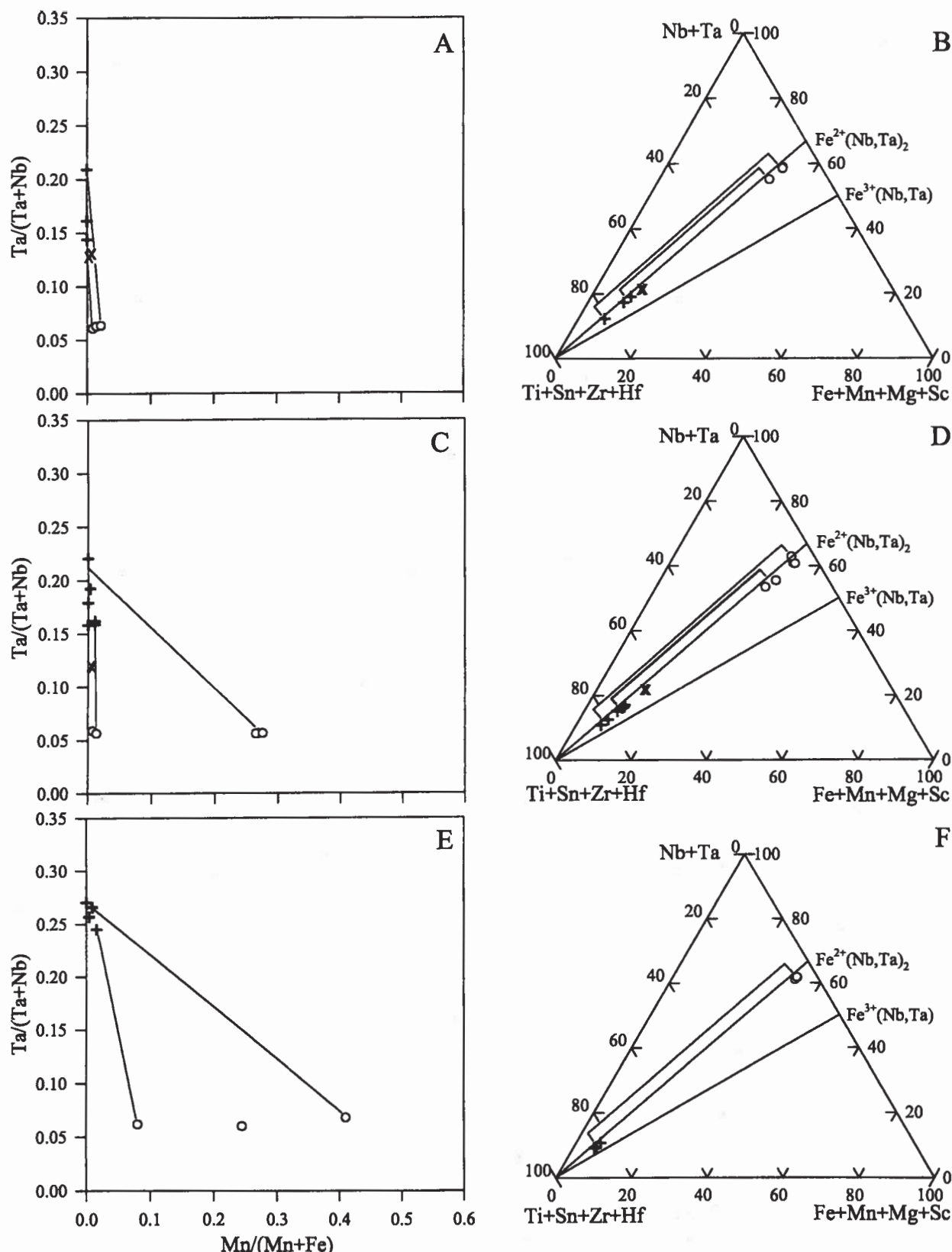


Fig. 3. Selected examples of progressive stages of exsolution in the Věžná I niobian rutile I in the columbite quadrilateral and in the $(\text{Nb}+\text{Ta}) - (\text{Ti}+\text{Sn}+\text{Zr}+\text{Hf}) - (\text{Fe}_{\text{tot}} + \text{Mn} + \text{Mg} + \text{Sc})$ diagram: A, B – incipient very fine-grained exsolution (cf. Fig. 1A, B); C, D – predominant, intermediate degree of exsolution (cf. Fig. 1E); E, F – coarse-grained products of advanced exsolution (similar to those shown in Fig. 1F). Graphic symbols as in Fig. 2. Tie-lines (in A, C, E) and brackets (in B, D, F) connect pairs of coexisting rutile matrix and exsolved ferrocolumbite grain. Note the gradual enrichment of rutile in Ta, and the Nb-rich plus progressively Mn-enriched composition of ferrocolumbite demonstrated in the quadrilaterals, and the trend toward pure rutile and columbite evident in the ternary diagrams.

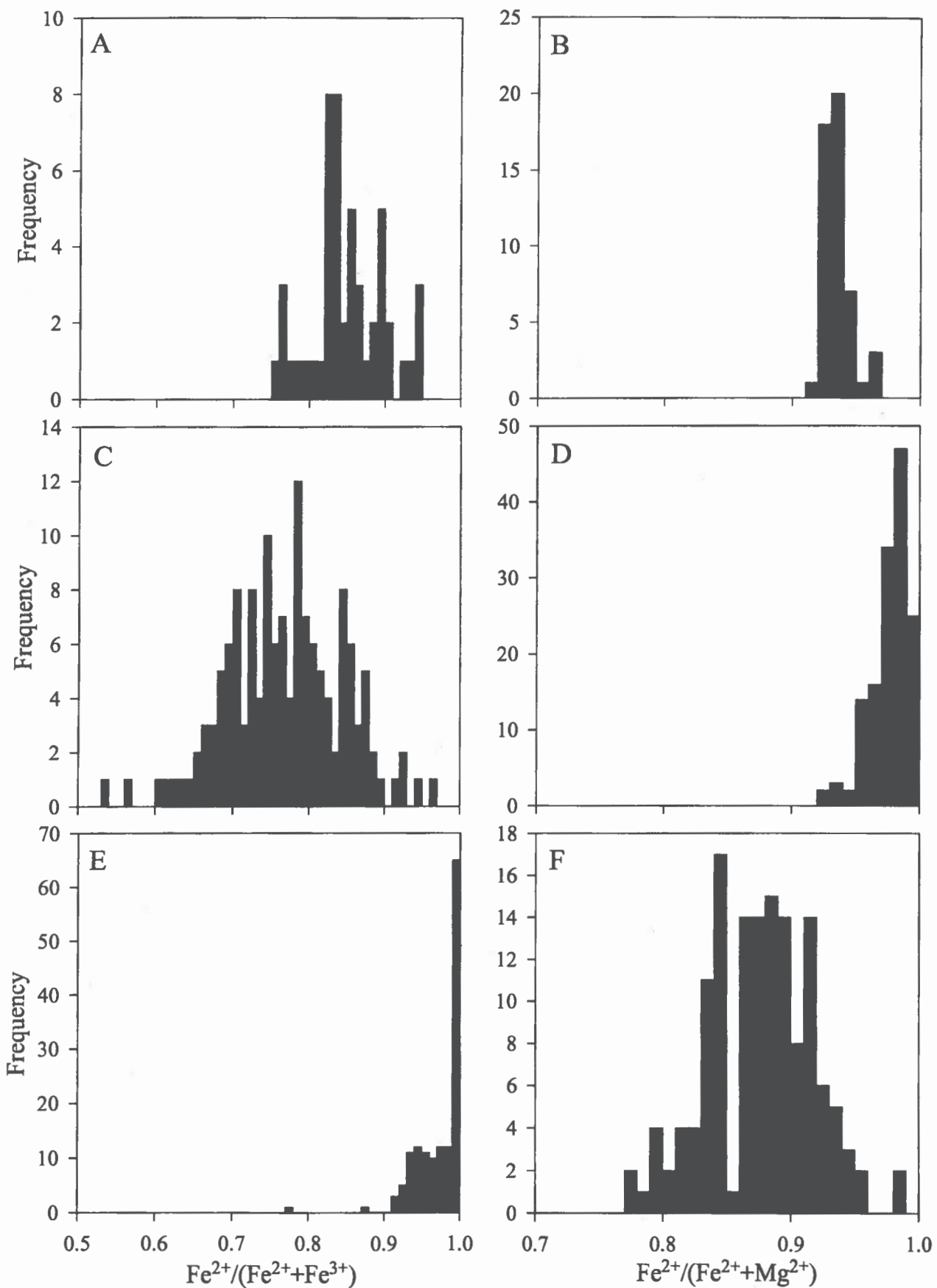


Fig. 4. Histograms of $\text{Fe}^{2+}/(\text{Fe}^{2+}+\text{Fe}^{3+})$ and $\text{Fe}^{2+}/(\text{Fe}^{2+}+\text{Mg})$ in the primary homogeneous niobian rutile I (A and B), depleted rutile I (C and D), and exsolved titanian ferrocolumbite I (E and F); all data in atomic ratios. Exsolution leads to preferential partitioning of Fe^{3+} into the rutile phase, and of Mg into the ferrocolumbite phase. Distributions of Sc, W and Ca show partition analogous to that of Mg.

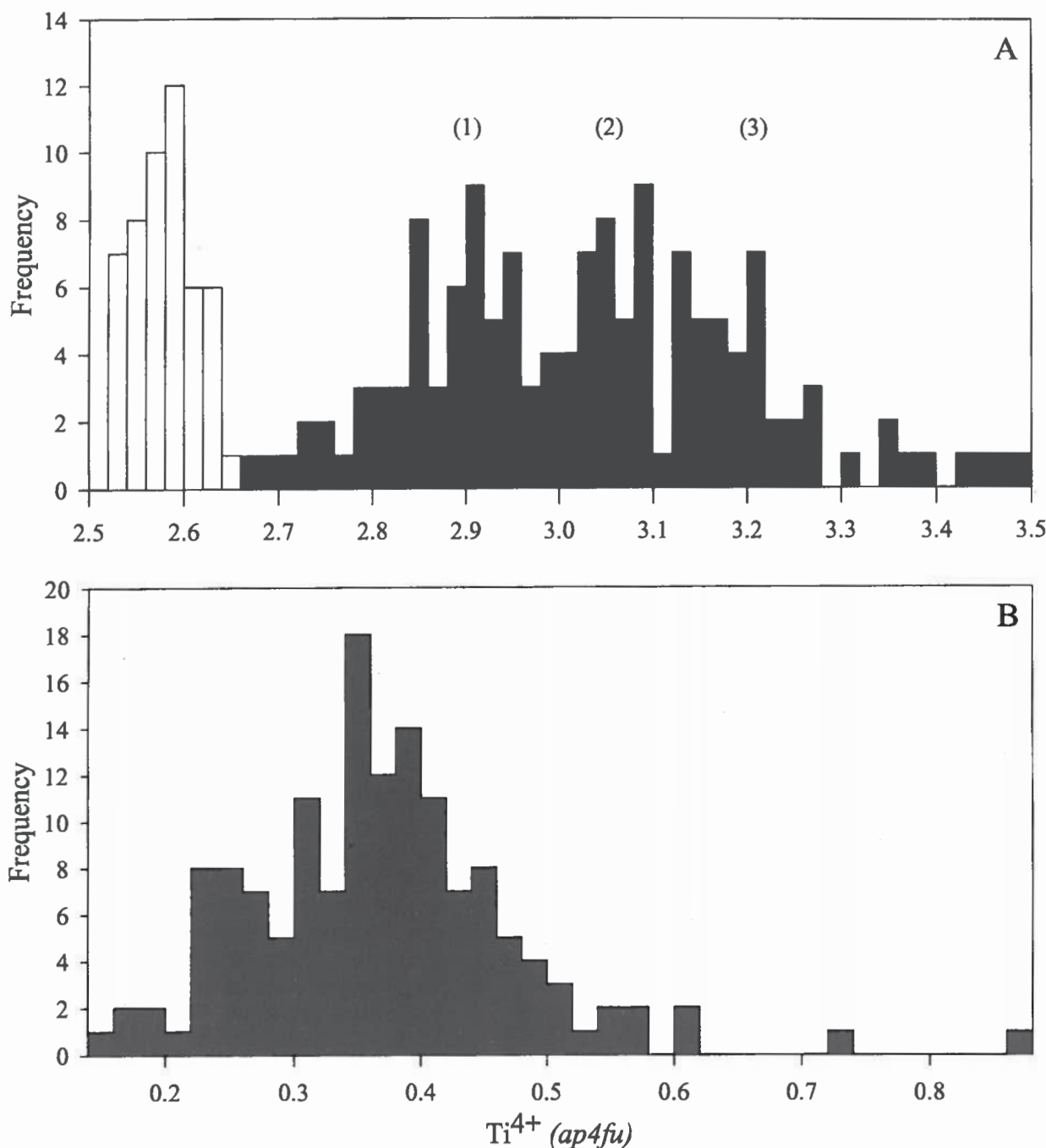


Fig. 5. Histograms of Ti^{4+} contents in primary homogeneous (white) and depleted (black) niobian rutile I (A) and exsolved titanian ferrocolumbite I (B). Note the simple near-Gaussian distribution of Ti in the primary niobian rutile and in the exsolved columbite phase, but the quasi-trimodal distribution in the medium-depleted niobian rutile I, with maxima at about 2.90, 3.05 and 3.18 Ti^{4+} apfu (close to 62.5, 67.5 and 72 wt. % TiO_2 , respectively).

Niobian rutile II and titanian ferrocolumbite II

Granular aggregates of depleted niobian rutile II and exsolved ferrocolumbite II rarely accompany scarce pods of the late, Li, Rb, Cs-enriched mineral association described sub “The parent pegmatite and mineral assemblages”. Grains located within 2 cm of the lepidolite + elbaite + pollucite aggregates show compositions of the rutile II and ferrocolumbite II phases (Ta-

ble 5, Fig. 2C, G) similar to those of the most exsolved and Mn-enriched type I. The coarse texture of the exsolution intergrowth and the absence of a homogeneous primary rutile phase also are similar to the features of the most evolved niobian rutile I + ferrocolumbite I pairs (Fig. 1F). The W content of ferrocolumbite II and the Sn content of rutile II are the highest ever encountered in any generation of these phases in the Věžná I pegmatite.

Table 4. Chemical compositions representative of the most exsolved and coarsest-grained intergrowths of depleted niobian rutile I (R) and ferrocolumbite I (FC) from the Věžná I pegmatite. Atomic contents based on 8 oxygen atoms and 4 cations (see "Experimental" for details). The data correspond to some of those shown in Figs 3E, F, and are similar to compositions characteristics of the two phases in Fig. 1F.

	A61A-2 R	A61A-4 R	A61A-5 R	A61A-3 FC	A61A-7 FC	A61A-6 FC
WO ₃	0.40	0.04	0.06	3.16	4.30	4.36
Nb ₂ O ₅	12.12	10.65	10.28	64.99	65.96	64.39
Ta ₂ O ₅	6.55	6.55	6.20	7.12	7.00	7.77
TiO ₂	73.69	77.18	77.92	4.02	3.56	3.46
ZrO ₂	0.00	0.00	0.00	0.00	0.00	0.00
HfO ₂	0.00	0.00	0.00	0.01	0.00	0.00
SnO ₂	1.03	1.01	1.04	0.38	0.25	0.30
ThO ₂	0.00	0.00	0.01	0.00	0.00	0.00
UO ₂	0.00	0.00	0.00	0.02	0.00	0.06
Sc ₂ O ₃	0.00	0.00	0.00	0.48	0.80	0.41
Fe ₂ O ₃	1.71	2.32	1.86	0.40	0.00	0.00
As ₂ O ₃	0.00	0.00	0.00	0.00	0.00	0.00
Y ₂ O ₃	0.01	0.01	0.03	0.04	0.09	0.06
Sb ₂ O ₃	0.00	0.07	0.00	0.04	0.00	0.01
Bi ₂ O ₃	0.04	0.00	0.10	0.13	0.00	0.00
MgO	0.05	0.04	0.05	1.25	1.19	1.11
CaO	0.00	0.02	0.00	0.01	0.02	0.08
MnO	0.08	0.01	0.04	1.38	4.17	7.10
FeO	3.46	2.73	2.79	15.59	13.02	10.35
ZnO	0.06	0.01	0.00	0.00	0.00	0.02
PbO	0.00	0.14	0.08	0.00	0.00	0.00
TOTAL	99.20	100.78	100.46	99.02	100.36	99.48
W	0.006	0.001	0.001	0.063	0.084	0.087
Nb	0.324	0.278	0.268	2.252	2.260	2.241
Ta	0.105	0.103	0.097	0.148	0.144	0.163
Ti	3.280	3.353	3.384	0.232	0.203	0.200
Zr	0.000	0.000	0.000	0.000	0.000	0.000
Hf	0.000	0.000	0.000	0.000	0.000	0.000
Sn	0.024	0.023	0.024	0.012	0.008	0.009
Th	0.000	0.000	0.000	0.000	0.000	0.000
U	0.000	0.000	0.000	0.000	0.000	0.001
Sc	0.000	0.000	0.000	0.032	0.053	0.027
Fe ³⁺	0.076	0.101	0.081	0.023	0.000	0.000
As	0.000	0.000	0.000	0.000	0.000	0.000
Y	0.000	0.000	0.001	0.002	0.004	0.002
Sb	0.000	0.002	0.000	0.001	0.000	0.000
Bi	0.001	0.000	0.001	0.003	0.000	0.000
Mg	0.004	0.003	0.004	0.143	0.134	0.127
Ca	0.000	0.001	0.000	0.001	0.002	0.007
Mn	0.004	0.000	0.002	0.090	0.268	0.463
Fe ²⁺	0.172	0.132	0.135	1.000	0.825	0.666
Zn	0.003	0.000	0.000	0.000	0.000	0.001
Pb	0.000	0.002	0.001	0.000	0.000	0.000

Niobian rutile III and titanian ferrocolumbite III

In contrast to the preceding generations, these phases form discrete subhedral to euhedral stubby crystals 0.1 to 0.5 mm in size, perched on euhedral quartz lining fissures in quartzo-feldspathic matrix. Closely associated as they are, the two minerals were not observed in mutual contact or any kind of intergrowth. Within individual crystals, each phase is homogeneous in BSE images, although rutile is somewhat variable in terms of Ta/(Ta+Nb) and ferrocolumbite shows a relatively broad range of Mn/(Mn+Fe) (Table 6, Figure 2D, H). The (Fe, Nb, Ta)-component of rutile III is quite subordinate, and so is the Ti content of

the associated ferrocolumbite III. The contents of Sc are much lower than in the niobian rutile I and its exsolution products, and the Zr and Hf contents are below detection limits. In contrast, SnO₂ is much higher (up to 1.73 wt. % in niobian rutile III), although lower than in the niobian rutile II.

As was the case with niobian rutile I and ferrocolumbite I exsolutions pairs, niobian rutile III shows a monorutile structure, and the titanian ferrocolumbite III displays a disordered structural state. On heating to 1000 °C for 16 h. in air, the disordered ferrocolumbite III converts to a cation-ordered columbite structure.

Discussion

The Věžná I niobian rutile is a typical representative of the compositional type of this phase which is characterized by strong dominance of Fe²⁺ over Fe³⁺. Such niobian rutile almost invariably exsolves into a Nb, Ta, Fe-depleted rutile and titanian ferrocolumbite (e. g., Sahama 1978, Černý et al. 1981), in contrast to niobian rutile containing about equal concentrations of divalent and trivalent Fe (Černý et al. 1999) or dominant (Fe, Sc)³⁺ (Černý et al. 2000). Abundant data on the primary niobian rutile I, its exsolution products, and later generations of niobian rutile II and III permit a thorough discussion of the Věžná case in terms of crystal chemistry (with implications for Fe²⁺-dominant niobian rutile in general) and in terms of phase evolution during consolidation of the parent pegmatite (specific for Věžná I).

Crystal chemistry of the rutile phase

Primary niobian rutile I seems to incorporate substantial quantities of Nb and Fe, minor Ta, and negligible Mn plus Mg via the substitution (Fe, Mn, Mg)²⁺₊₁(Nb, Ta)⁵⁺₊₂Ti⁴⁺₋₃. However, the entry of other cations with diverse valencies must be taken into account before the above substitution could be confirmed (except for homovalent substitution by Sn, Zr, Hf, U and Th). The cations in question include Fe³⁺, Sc³⁺, W⁶⁺, and the most likely substitution mechanisms are Fe³⁺₊₁(Nb, Ta)⁵⁺₊₁Ti⁴⁺₋₂, Sc³⁺₊₁(Nb, Ta)⁵⁺₊₁Ti⁴⁺₋₂, and (Fe, Mn, Mg)²⁺₊₂W⁶⁺₊₁Ti⁴⁺₋₂, respectively. Figure 6 shows the plots of all generations of niobian rutile adjusted for the above minor substitutions, with excellent correlation of the terms (Fe²⁺+Mn+Mg-W) and (Nb+Ta-Fe³⁺-Sc) lined up along the 1:2 ratio. This confirms both the principal mechanism of incorporation of divalent and pentavalent cations, and the validity of the substitutions assumed for the minor cations.

Crystal chemistry of the ferrocolumbite phase

Ferrocolumbite exsolved from niobian rutile I and II, and coprecipitated with niobian rutile III, contains substantial Fe, Mn, and Nb dominant over subordinate Ta. Ferrocolumbite also shows considerable substitution by Mg, Sc, Fe³⁺, Ti, W and minor Zr plus Hf and Ca. The incor-

Table 5. Chemical composition of niobian rutile II and ferrocolumbite II from the Věžná I pegmatite (cf. Fig. 2C, G). Atomic on 8 oxygen atoms and 4 cations (see "Experimental" for details).

	G1–1 R	G1–5 R	G3brt R	G1–8 FC	G1–11 FC	G2–3 FC
WO ₃	0.00	0.67	0.58	4.95	7.23	4.14
Nb ₂ O ₅	13.34	18.22	20.90	59.69	57.70	60.80
Ta ₂ O ₅	6.81	7.00	7.24	7.16	6.96	6.87
TiO ₂	71.91	64.22	61.62	6.49	6.29	6.43
ZrO ₂	0.00	0.00	0.00	0.06	0.07	0.15
HfO ₂	0.00	0.00	0.00	0.04	0.00	0.00
SnO ₂	1.48	2.53	1.72	1.38	1.10	0.55
ThO ₂	0.00	0.00	0.07	0.00	0.00	0.00
UO ₂	0.04	0.00	0.07	0.00	0.10	0.02
Sc ₂ O ₃	0.00	0.00	0.06	0.79	0.94	1.54
Fe ₂ O ₃	2.58	1.32	1.07	1.27	0.67	1.42
As ₂ O ₃	0.02	0.01	0.00	0.00	0.00	0.00
Y ₂ O ₃	0.00	0.00	0.02	0.01	0.10	0.04
Sb ₂ O ₃	0.06	0.02	0.00	0.02	0.00	0.00
Bi ₂ O ₃	0.00	0.04	0.12	0.00	0.01	0.00
MgO	0.01	0.02	0.02	0.19	0.40	0.58
CaO	0.01	0.02	0.01	0.04	0.03	0.01
MnO	0.03	0.03	0.07	0.39	6.24	4.81
FeO	3.47	5.57	6.35	17.05	11.04	11.46
ZnO	0.00	0.00	0.00	0.00	0.03	0.00
PbO	0.00	0.00	0.00	0.00	0.00	0.00
TOTAL	99.76	99.67	99.92	99.54	98.92	98.82

W	0.000	0.011	0.009	0.098	0.145	0.082
Nb	0.357	0.504	0.582	2.065	2.021	2.093
Ta	0.110	0.116	0.121	0.149	0.147	0.142
Ti	3.205	2.955	2.855	0.374	0.366	0.368
Zr	0.000	0.000	0.000	0.002	0.003	0.006
Hf	0.000	0.000	0.000	0.001	0.000	0.000
Sn	0.035	0.062	0.042	0.042	0.034	0.017
Th	0.000	0.000	0.001	0.000	0.000	0.000
U	0.001	0.000	0.001	0.000	0.002	0.000
Sc	0.000	0.000	0.003	0.053	0.063	0.102
Fe ³⁺	0.115	0.061	0.049	0.073	0.039	0.081
As	0.001	0.000	0.000	0.000	0.000	0.000
Y	0.000	0.000	0.001	0.000	0.004	0.002
Sb	0.001	0.001	0.000	0.001	0.000	0.000
Bi	0.000	0.001	0.002	0.000	0.000	0.000
Mg	0.001	0.002	0.002	0.022	0.046	0.066
Ca	0.001	0.001	0.001	0.003	0.002	0.001
Mn	0.002	0.002	0.004	0.025	0.409	0.310
Fe ²⁺	0.172	0.285	0.327	1.092	0.716	0.730
Zn	0.000	0.000	0.000	0.000	0.002	0.000
Pb	0.000	0.000	0.000	0.000	0.000	0.000

poration of Mg²⁺ and Ca²⁺ is undoubtedly homovalent for (Fe,Mn)²⁺, and the entry of Fe³⁺ and Sc³⁺ can be envisaged via (Fe,Sc)³⁺₃ (Nb,Ta)⁵⁺₃ (Fe,Mn,Mg,Ca)²⁺₋₂ (Nb,Ta)⁵⁺₋₄. The substitution by Ti and minor Zr plus Hf can be expected to be accomplished mainly, if not exclusively, by the reversal of the main mechanism operating in niobian rutile, i. e. (Ti,Zr,Hf)⁴⁺₃ (Fe,Mn,Mg,Ca)²⁺₋₁ (Nb,Ta)⁵⁺₋₂. These assumptions are tested in Figure 7 by adjustments to the main substitution mechanism similar to those employed for niobian rutile, namely (Fe²⁺+Mn+Mg+Ca-W) vs (Nb+Ta-Fe³⁺-Sc). The correlation of the plotted data is very good and confirms both the main substitution by the tetravalent cations and the entry of the minor elements, as assumed above. However, a small portion of the data plots below the ideal 1:2 trend. Minor quantities of Y, Bi, Sb, As and Pb account to some

degree for these deviations but they do not eliminate them. Substitution mechanisms additional to the major substitutions quoted above may be involved (cf., e. g., Johan – Johan 1994), but their extent is negligible and out of reach of quantitative confirmation.

Figure 8A illustrates a positive correlation of Zr and Hf in the exsolved titanian ferrocolumbite I, similar to that recognized for this pair of coherent elements in ex-solutions of wodginite in cassiterite (Masau et al. 2000). However, the correlation coefficient of 0.388 is very low: this is undoubtedly due to high analytical error on the part of Hf, as most of the determined contents are close to the quantitative detection limit of the EMPA conditions employed. Nevertheless, our results on ferrocolumbite

Table 6. Representative chemical compositions of discrete crystals of niobian rutile III and titanian ferrocolumbite III from quartz-coated fissures of the Věžná I pegmatite (cf. Fig. 2D, H). Atomic contents based on 8 oxygen atoms and 4 cations (see "Experimental" for details). Note the similarity to the compositions of the most advanced exsolution products of niobian rutile I (Table 4).

	V1–3 R	V2–3 R	V2–7 R	V1–2 FC	V2–1 FC	V2–2 FC
WO ₃	0.00	0.22	0.21	4.09	4.77	3.55
Nb ₂ O ₅	8.96	9.08	9.06	62.77	61.24	62.96
Ta ₂ O ₅	6.58	6.58	6.43	8.19	9.29	9.65
TiO ₂	76.95	76.92	76.95	3.65	3.29	3.03
ZrO ₂	0.00	0.00	0.00	0.00	0.00	0.00
HfO ₂	0.00	0.00	0.00	0.00	0.00	0.00
SnO ₂	1.69	1.56	1.52	0.69	0.51	0.57
ThO ₂	0.00	0.06	0.00	0.00	0.01	0.00
UO ₂	0.00	0.01	0.03	0.11	0.02	0.10
Sc ₂ O ₃	0.00	0.00	0.00	0.50	0.26	0.31
Fe ₂ O ₃	1.66	1.05	1.05	0.00	0.00	0.00
As ₂ O ₃	0.03	0.01	0.01	0.00	0.00	0.00
Y ₂ O ₃	0.00	0.04	0.01	0.02	0.05	0.04
Sb ₂ O ₃	0.00	0.00	0.01	0.00	0.00	0.00
Bi ₂ O ₃	0.04	0.00	0.04	0.00	0.00	0.06
MgO	0.04	0.03	0.03	0.78	0.71	0.69
CaO	0.00	0.01	0.01	0.02	0.03	0.04
MnO	0.01	0.02	0.00	6.27	8.47	8.72
FeO	2.61	3.00	3.00	11.38	9.39	9.35
ZnO	0.00	0.02	0.00	0.00	0.00	0.00
PbO	0.12	0.01	0.03	0.00	0.00	0.00
TOTAL	98.69	98.61	98.39	98.47	98.04	99.07
W	0.000	0.003	0.003	0.083	0.098	0.072
Nb	0.238	0.242	0.242	2.216	2.191	2.226
Ta	0.105	0.105	0.103	0.174	0.200	0.205
Ti	3.407	3.410	3.416	0.214	0.196	0.178
Zr	0.000	0.000	0.000	0.000	0.000	0.000
Hf	0.000	0.000	0.000	0.000	0.000	0.000
Sn	0.040	0.037	0.036	0.021	0.016	0.018
Th	0.000	0.001	0.000	0.000	0.000	0.000
U	0.000	0.000	0.000	0.002	0.000	0.002
Sc	0.000	0.000	0.000	0.034	0.018	0.021
Fe ³⁺	0.073	0.046	0.047	0.000	0.000	0.000
As	0.001	0.000	0.000	0.000	0.000	0.000
Y	0.000	0.001	0.000	0.001	0.002	0.002
Sb	0.000	0.000	0.000	0.000	0.000	0.000
Bi	0.001	0.000	0.001	0.000	0.000	0.001
Mg	0.004	0.003	0.003	0.091	0.084	0.080
Ca	0.000	0.001	0.001	0.002	0.003	0.003
Mn	0.000	0.001	0.000	0.415	0.568	0.578
Fe ²⁺	0.128	0.148	0.148	0.743	0.621	0.612
Zn	0.000	0.001	0.000	0.000	0.002	0.000
Pb	0.002	0.000	0.000	0.000	0.000	0.000

(combined with Zr detected in niobian rutile; Table 1) confirm the data of Michailidis (1997), and the first Věžná data obtained by Novák – Černý (1998), which indicate that trace to subordinate amounts of Zr and Hf are incorporated not only into cassiterite (Möller – Dulski 1983, Masau et al. 2000) but into rutile as well. On exsolution, both elements migrate into a complex oxide phase. Preliminary data suggest that the Zr/Hf ratio in the Věžná I exsolved ferrocolumbite, averaging at 11.1, is close to that characteristic of zircon associated with the primary homogeneous niobian rutile I.

Figure 8B indicates that Sc is not linked to Fe^{3+} and Sc in the Věžná titanian ferrocolumbite I, and the limited data available suggest that this link is also absent in the primary homogeneous niobian rutile I. This is in marked contrast to the behavior of Sc in numerous oth-

er geological environments (e. g., Wise et al. 1998, Novák – Černý 1998).

Element partitioning during exsolution

The data summarized in Tables 1 to 5 and illustrated in Figures 1 to 4 indicate a strong tendency of primary niobian rutile I and II to exsolve orthorhombic ferrocolumbite. With progress of exsolution, the parent tetragonal phase tends to eliminate most major and minor substituents, whereas the orthorhombic product of exsolution becomes Ti-poor. This is in general agreement with the stability relationships in the columbite group *sensu lato*, marked by the rutile structure of FeTa_2O_6 but a columbite-type orthorhombic architecture of MnTa_2O_6 and both Nb-dominant end-members (Brandt 1943, Černý – Ercit

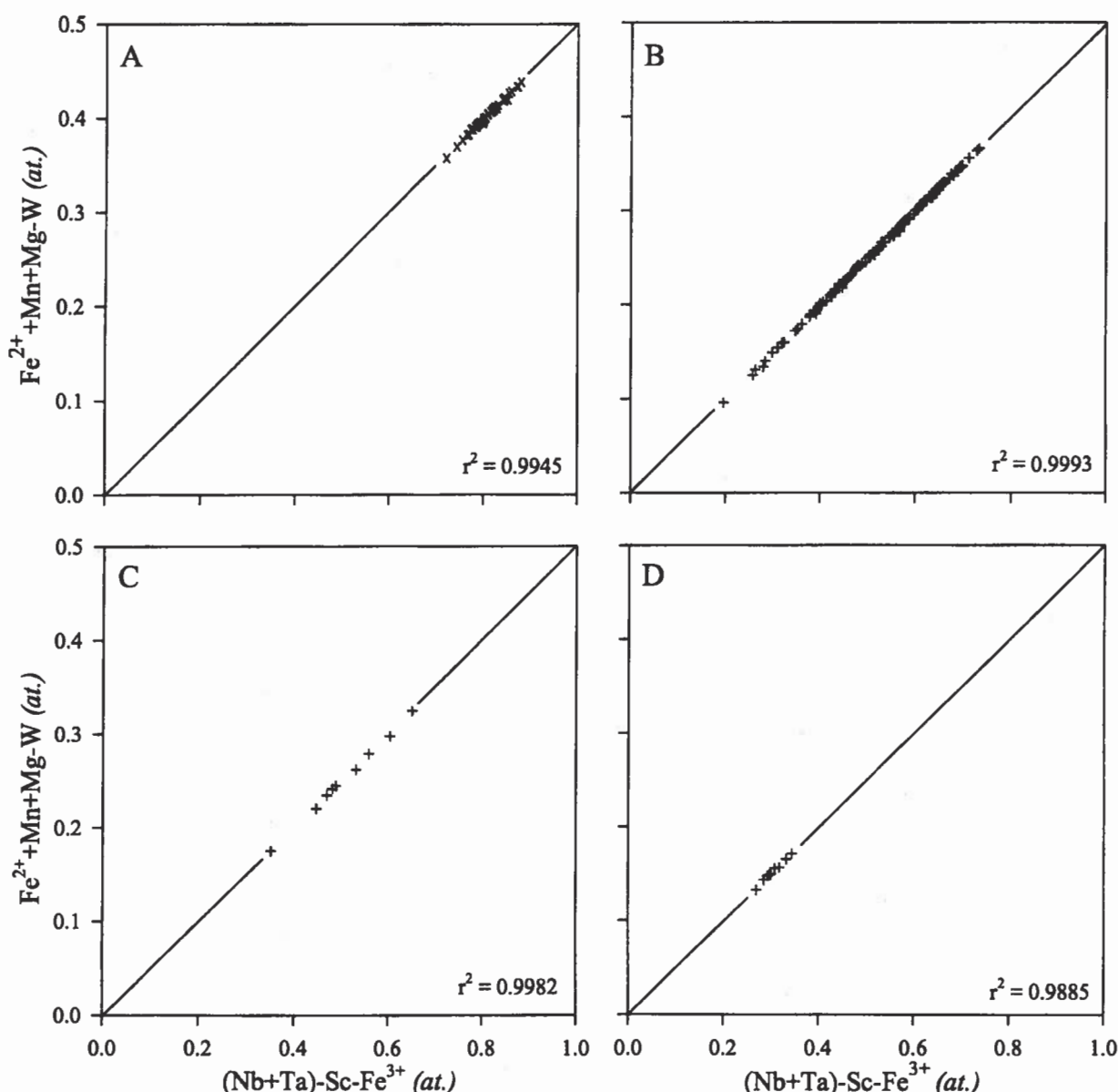


Fig. 6. Virtually perfect correlation of the terms $(\text{Fe}^{2+} + \text{Mn} + \text{Mg} - \text{W})$ and $(\text{Nb} + \text{Ta} - \text{Sc} - \text{Fe}^{3+})$ in primary homogeneous niobian rutile I (A), depleted niobian rutile I (B), depleted niobian rutile II (C) and niobian rutile III (D).

1989). As demonstrated earlier, tantalian rutile generally remains stable on cooling (as do some Nb-poor cases of niobian rutile), but niobian rutile with substantial extent of substitution invariably breaks down to an intergrowth of depleted rutile and exsolved titanian ferrocolumbite or ixiolite (Černý et al. 1981, Černý – Ercit 1989).

The structure of the orthorhombic phase proves to be much more flexible and accomodating for a variety of subordinate to minor substituents than that of rutile. Ferrocolumbite clearly becomes a sink for Mg, Mn, Fe²⁺, Fe³⁺, Sc, Zr, Hf, U, Nb, Ta and W, whereas rutile conserves only Sn and Ta. In relative terms, rutile retains Ta, Fe²⁺ and Fe³⁺, with preference for the latter, and ferrocolumbite extracts mainly Mn and Nb.

Course of crystallization and breakdown

Primary homogeneous niobian rutile I rarely shows diffuse streaks enriched in Nb, Ta, Sc, Fe and Mn, possibly still in structural continuity with the surrounding rutile matrix. In most cases, fine-grained exsolution of orthorhombic ferrocolumbite I is the characteristic first product of breakdown, which substantially depletes the rutile phase of the substituting elements. Coarse aggregates of ferrocolumbite directly adjacent to primary homogeneous rutile are rather exceptional.

With continuing exsolution, presumably during gradual temperature decrease, the compositional differences between the rutile and ferrocolumbite phases increase. Distribution of Ti in depleted rutile I suggests that the exsolution could have proceeded in several, possibly temperature-controlled steps.

In some samples which lack relics of primary homogeneous niobian rutile, the titanian ferrocolumbite shows

considerable enrichment in Mn. Considering the modal proportions of rutile to ferrocolumbite in these samples (~4:1), it is obvious that the parent homogeneous phase must have been distinctly enriched in Mn relative to the relics of primary homogeneous niobian rutile in the Mn-poor assemblages. It is conceivable that such a Mn-rich tetragonal phase would be even less stable than the strongly Fe-dominant compositions, and would become completely exsolved (see Weitzel 1976, Lahti et al. 1983, Černý – Ercit 1989 concerning metastability of manganotapiolite, and Masau et al. 2000 about the breakdown of manganan-tantalum cassiterite).

The niobian rutile I + Mn-enriched ferrocolumbite I pairs came from samples which were not collected *in situ* in the pegmatite outcrop. Consequently, their position in space and time relative to the niobian rutile I + Mn-poor ferrocolumbite I cannot be ascertained. Nevertheless, it can be assumed on geochemical grounds that the Mn-enriched (and possibly Ta-enriched) primary rutile represented a relatively late product of fractional crystallization.

This is supported by the phase relations and chemical compositions of the depleted niobian rutile II + Mn-rich ferrocolumbite II. These exsolution intergrowths, also free of relics of the primary homogeneous niobian rutile, are quite analogous to the Mn-rich assemblage I, and they are located in immediate vicinity of the geochemically most evolved, Li, Rb, Cs, F-enriched silicate pods.

Late-stage enrichment of the Ti, Nb, Ta, Fe-bearing oxide assemblage in Mn is extended into the discrete but coexisting niobian rutile III and ferrocolumbite III, precipitated under low-temperature hydrothermal conditions in open fissures. The compositional similarity of the II, III and some cases of the I generation of the oxide min-

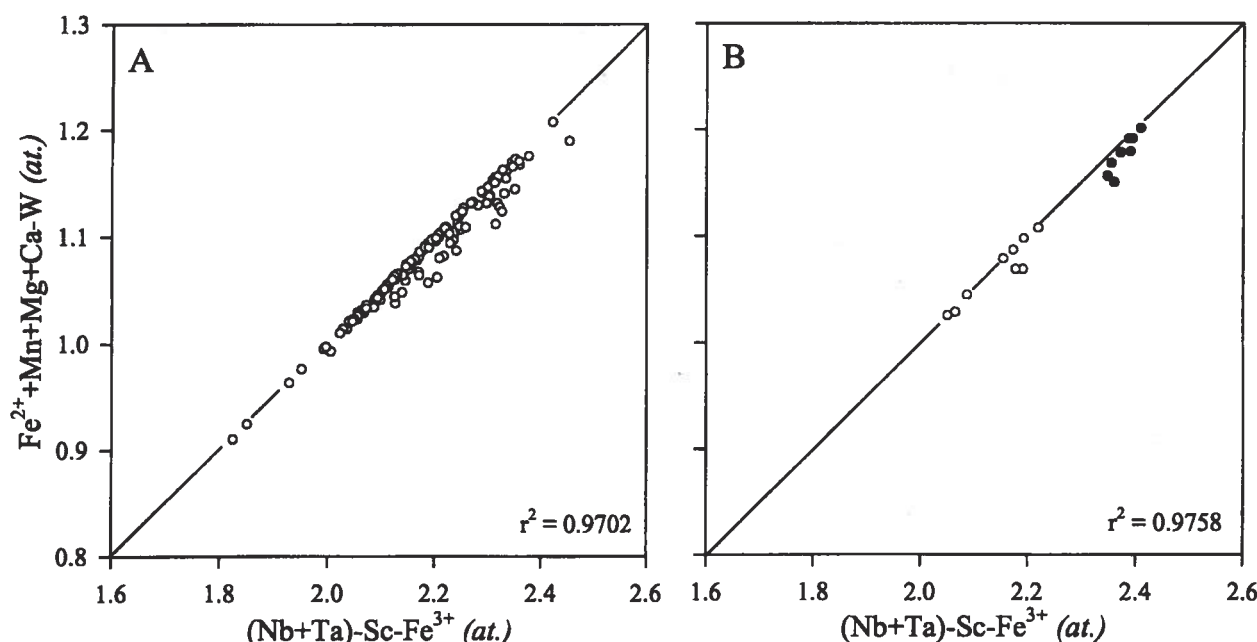


Fig. 7. Correlation of the terms $(\text{Fe}^{2+}+\text{Mn}+\text{Mg}+\text{Ca}-\text{W})$ and $(\text{Nb}+\text{Ta}-\text{Sc}-\text{Fe}^{3+})$ in titanian ferrocolumbite I (A), II (open circles) and III (solid dots) (B). See text for discussion of deviating data points.

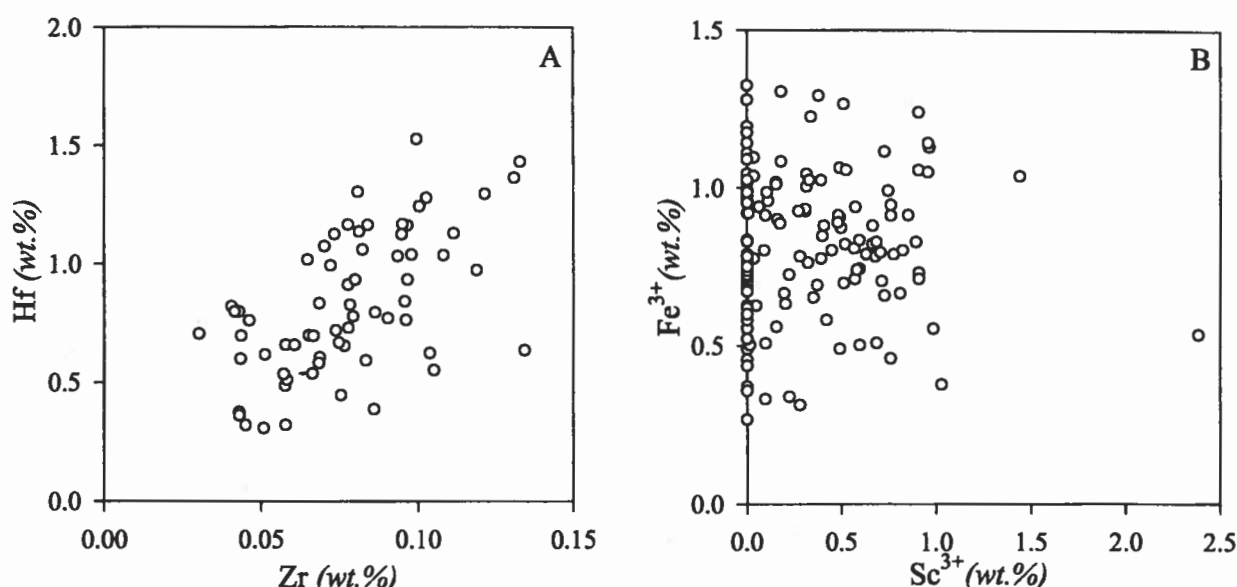


Fig. 8. Correlation of Zr vs. Hf (A) and Sc vs. Fe^{3+} (B) in the titanian ferrocolumbite exsolved from niobian rutile I. Note a rough but distinct correlation of Hf with Zr, but a total lack of any relationship between Sc and Fe^{3+} .

erals suggests that the III pair could have been mobilized and redeposited from the earlier assemblages; coarse exsolution intergrowths I are locally porous and probably leached.

Summary

Niobian rutile crystallized in the Věžná I pegmatite in three generations: niobian rutile I associated with beryllian cordierite, beryl, zircon, xenotime-(Y) and monazite-(Ce), transitional into niobian rutile II in close vicinity of small pollucite-, lepidolite- and elbaite-bearing pods, and niobian rutile III in fissures with ferrocolumbite III, niobian titanite and pyrochlore-microlite. Exsolution of the niobian rutile I and II into depleted rutile and titanian ferrocolumbite is extensive. Exsolution possibly proceeded in several, presumably temperature-controlled stages. Relics of primary homogeneous niobian rutile are preserved in most crystals of generation I, but some of them and those of generation II, all perceptibly enriched in Mn, are completely exsolved. Oxide minerals of the last generation III could have been mobilized and redeposited from compositionally similar, porous aggregates of intergrowths I and II.

Heterovalent substitutions in niobian rutile are accomplished by $(\text{Fe}, \text{Mn}, \text{Mg})^{2+}_{+1} (\text{Nb}, \text{Ta})^{5+}_{+1} \text{Ti}^{4+}_{-2}$, $\text{Fe}^{3+}_{+1} (\text{Nb}, \text{Ta})^{5+}_{+1} \text{Ti}^{4+}_{-2}$, $\text{Sc}^{3+}_{+1} (\text{Nb}, \text{Ta})^{5+}_{+1} \text{Ti}^{4+}_{-2}$, and by reverse mechanisms in ferro-columbite: $(\text{Fe}, \text{Sc})^{3+}_{+3} (\text{Nb}, \text{Ta})^{5+}_{+3} (\text{Fe}, \text{Mn}, \text{Mg}, \text{Ca})^{2+}_{-2}$, $(\text{Nb}, \text{Ta})^{5+}_{-4}$ and $(\text{Ti}, \text{Zr}, \text{Hf})^{4+}_{+3} (\text{Fe}, \text{Mn}, \text{Mg}, \text{Ca})^{2+}_{-1} (\text{Nb}, \text{Ta})^{5+}_{-2}$. Exsolution concentrates Mg, Mn, Fe^{2+} , Fe^{3+} , Sc, Zr, Hf, U, Nb, Ta and W in the exsolved ferrocolumbite. In relative terms, rutile conserves Sn, Fe^{2+} , Fe^{3+} , Ta, and Fe^{3+} relative to Fe^{2+} , whereas Mn and Nb are preferred by the columbite structure.

Considerable concentration of Zr and Hf in exsolved ferrocolumbite and low Zr content of undepleted niobian rutile confirm that Zr and Hf must be considered significant minor elements in niobian rutile from granitic environments. Considerable enrichment in Mg can be presumed a local feature, reflecting contamination of the pegmatite by serpentinite wallrock.

Acknowledgements. This work was supported by the Natural Sciences and Engineering Research Council of Canada Major Installation, Equipment, Infrastructure and Research Grants to PČ and F. C. Hawthorne, and by the Faculty of Science (University of Manitoba) Postdoctoral Fellowship to MN. The authors are indebted to Dr. D. K. Teertstra for assistance in X-ray diffraction work, and to J. Kjellman and Dr. Wm. B. Simmons for thorough reviews of the manuscript.

Submitted October 12, 1999

References

- Appleman, D. E. – Evans, H. T. Jr. (1973): Job 9214: Indexing and least-squares refinement of powder diffraction data. – U. S. Nat. Techn. Inf. Service, Document PB 216–188.
- Brandt, K. (1943): X-ray studies on ABO_4 compounds of rutile type and AB_2O_6 compounds of columbite type. – Arkiv Kemi, Mineral., Geol., 17A, 15, 1–8.
- Čech, F. (1963): Contributions to the mineralogy of Moravia and Silesia. – Acta. Mus. Moraviae, Sci. Nat., 58, 31–42 (in Czech).
- Čech, F. – Černý, P. – Povondra, P. (1964): Ilmenorutile from Údraž, near Písek, and its disintegration products. – Acta Univ. Carolinae – Geol., 1964, 1, 1–14 (in Czech).
- Černý, P. (1960): Milarite and wellsite from Věžná. – Acta Acad. Sci. Cechosl., Basis Brunensis, 32, 1, 399, 1–16 (in Czech).
- Černý, P. (1968): Berylliummineral in Pegmatiten von Věžná und ihre Umwandlungen. Berichte deutsch. Ges. geol. Wiss., R. B. Miner. Lagerstättenf., 13, 565–578 (in German).

- Černý, P. – Čech, F.* (1962): Ilmenorutile from Věžná in western Moravia and the products of its breakdown. – *Acta Mus. Moraviae*, 47, 13–22 (in Czech).
- Černý, P. – Čech, F. – Povondra, P.* (1964): Review of ilmenorutile – struvite minerals. – *N. Jahrb. Mineral., Abh.*, 101, 142–172.
- Černý, P. – Chapman, R. – Masau, M.* (2000): Two-stage exsolution of a titanian (Sc,Fe^{3+}) $(\text{Nb},\text{Ta})\text{O}_4$ phase in Norwegian niobian rutile. – *Can. Mineral.*, submitted.
- Černý, P. – Chapman, R. – Simmons, W. B. – Chackowsky, L. E.* (1999): Niobian rutile from the McGuire granitic pegmatite, Park County, Colorado: Solid solution, exsolution, and oxidation. – *Amer. Mineral.*, 84, 754–763.
- Černý, P. – Ercit, T. S.* (1989): Mineralogy of niobium and tantalum: crystal-chemical relationships, paragenetic aspects and their economic implications. – In: P. Möller – P. Černý – F. Saupé (eds.) *Lanthanides, Tantalum and Niobium*, Springer-Verlag, 27–79.
- Černý, P. – Hawthorne, F. C. – Jarosewich, E.* (1980): Crystal chemistry of milarite. *Can. Mineral.* 18, 41–57.
- Černý, P. – Miškovský, J.* (1966): Ferroan phlogopite and magnesian vermiculite from Věžná, western Moravia. – *Acta Univ. Carolinae – Geol.*, 1966, 17–32.
- Černý, P. – Novák, M.* (1992): Locality No. 2: Věžná near Nedvědice, a pegmatite dike of the beryl-columbite subtype penetrating serpentinite. – In: *Field Trip Guidebook, Lepidolite 200 Symposium, Nové Město na Moravě*, 27–32.
- Černý, P. – Novák, M. – Chapman, R.* (1992): The $\text{Al}(\text{Nb},\text{Ta})\text{Ti}_{2-}$ substitution in titanite: the emergence of a new species? – *Mineral. Petrol.*, 52, 61–73.
- Černý, P. – Paul, B. J. – Hawthorne, F. C. – Chapman, R.* (1981): A niobian rutile – disordered columbite intergrowth from the Huron Claim pegmatite, southeastern Manitoba. – *Can. Mineral.*, 19, 541–548.
- Černý, P. – Povondra, P.* (1966): Beryllian cordierite from Věžná: $(\text{Na},\text{K}) + \text{Be} \rightarrow \text{Al}$. – *N. Jahrb. Mineral., Monatsh.*, 1966, 36–44.
- Černý, P. – Turnock, A. C.* (1971): Niobium-tantalum minerals from granitic pegmatites at Greer Lake, southeastern Manitoba. – *Can. Mineral.*, 10, 755–772.
- Ercit, T. S. – Černý, P. – Hawthorne, F. C. – McCammon, C. A.* (1992): The wodginite group. II. Crystal chemistry. – *Can. Mineral.*, 30, 613–631.
- Ercit, T. S. – Wise, M. A. – Černý, P.* (1995): Compositional and structural systematics of the columbite group. – *Amer. Mineral.*, 80, 613–619.
- Hawthorne, F. C. – Kimata, M. – Černý, P. – Ball, N. – Rossman, G. R. – Grice, J. D.* (1991): The crystal chemistry of the milarite-group minerals. – *Amer. Mineral.*, 76, 1836–1856.
- Johan, Z. – Johan, V.* (1994): Accessory minerals of the Cinovec (Zinnwald) granitic cupola, Czech Republic. I. Nb-, Ta- and Ti-bearing oxides. – *Mineral. Petrol.*, 51, 323–343.
- Lahti, S. I. – Johanson, B. – Virkkunen, M.* (1983): Contributions to the chemistry of tapiolite – manganotapiolite, a new mineral. – *Bull. Geol. Soc. Finland*, 55, 101–109.
- Masau, M. – Černý, P. – Chapman, R.* (2000): Exsolution of zirconian-hafnian wodginite from manganese-tantalum cassiterite, Annie Claim #3 granitic pegmatite, southeastern Manitoba. – *Can. Mineral.* (in press)
- Michailidis, K. M.* (1997): An EPMA and SEM study of niobian-tungsten rutile from the Fanos aplitic granite, Central Macedonia, Northern Greece. – *N. Jahrb. Mineral., Monatsh.* 1996, 549–563.
- Möller, P. – Dulski, P.* (1983): Fractionation of Zr and Hf in cassiterite. – *Chem. Geol.*, 40, 1–12.
- Novák, M. – Černý, P.* (1998): Scandium in columbite-group minerals from LCT pegmatites in the Moldanubicum, Czech Republic. – *Krytalnikum*, 24, 73–89.
- Novák, M. – Korbel, P. – Odehnal, F.* (1991): Pseudomorphs of bertrandite and epididymite after beryl from Věžná, Western Moravia, Czechoslovakia. – *N. Jahrb. Mineral., Monatsh.* 1991, 473–480.
- Novák, M. – Pelz, J.* (1981): Lithium-bearing pegmatite with pollucite from Věžná in western Moravia. – *Čas. Mineral. Geol.*, 26, 211–212 (in Czech).
- Pouchou, J. L. – Pichoir, F.* (1984): A new model for quantitative analysis. I. Application to the analysis of homogeneous samples. – *La Recherche Aerosp.*, 3, 13–38.
- Pouchou, J. L. – Pichoir, F.* (1985): "PAP" procedure for improved quantitative microanalysis. – *Microbeam Anal.* 1985, 104–106, San Francisco Press, San Francisco, California.
- Sahama, Th. G.* (1978): Niobian rutile from Muiane, Mozambique. – *Jornal de Mineral. Recife*, 7, 115–117.
- Teerstra, D. K. – Černý, P. – Novák, M.* (1995): Compositional and textural evolution of pollucite in pegmatites of the Moldanubicum. – *Mineral. Petrol.*, 55, 37–52.
- Weitzel, H.* (1976): Kristallstrukturverfeinerung von Wolframiten und Columbiten. – *Zeits. Krist.*, 144, 238–258.
- Wise, M. A. – Černý, P. – Falster, A. U.* (1998): Scandium substitution in columbite-group minerals and ixiolite. – *Can. Mineral.*, 36, 673–680.

Niobový rutil z Věžné: revize po 35 letech

Niobový rutil krystaloval v pegmatitu Věžná I ve třech generacích: niobový rutil I sdružený s berylnatým cordieritem, berylem, zirkonem, xenotitem-(Y), a monazitem-(Ce), přecházející do niobového rutilu II v těsné blízkosti malých hnězd s pollucitem, lepidolitem a elbaity, a niobový rutil III na puklinách společně s titanovým ferrocolumbitem III, niobovým titanitem a minerály ze skupiny mikrolitu – pyrochloru. Odmíšení niobového rutilu I a II na ochuzený rutil a titanový ferrocolumbit je velmi rozšířené. Odmíšení pravděpodobně proběhlo v několika fázích, kontrolovaných klesající teplotou. Relikty primárního homogenního niobového rutilu jsou zachovány ve většině kryštálů generace I, ale některé z nich jsou, podobně jako generace II, úplně odmíšeny; ve všech těchto případech se jedná o fáze zřetelně obohacené manganem. Koexistující oxidické minerály poslední III generace mohly být mobilizovány znova rekrystalovány z porezních, manganem obohacených agregátů generace II a III, jimž jsou svým složením blízké. Primární homogenní rutil obsahuje 34 až 38 mol. % ferrocolumbitové komponenty, a nepatrné množství $\text{Fe}^{3+}(\text{Nb},\text{Ta})\text{O}_4$. Obsah ferrocolumbitové složky v ochuzené rutilové fazi klesá až na 16 mol. %, zatímco obsah TiO_2 ve ferrocolumbitu klesá až na 5 mol. %. Heterovalentní substituce v niobovém rutilu jsou kontrolovány čtyřmi mechanismy: $(\text{Fe},\text{Mn},\text{Mg})^{2+}_{+1}(\text{Nb},\text{Ta})^{5+}_{+2}\text{Ti}^{4+}_{-3}\text{Fe}^{3+}_{+1}(\text{Nb},\text{Ta})^{5+}_{+1}\text{Ti}^{4+}_{-2}\text{Sc}^{3+}_{+1}(\text{Nb},\text{Ta})^{5+}_{+1}\text{Ti}^{4+}_{-2}$, a $(\text{Fe},\text{Mn},\text{Mg})^{2+}_{+1}\text{W}^{6+}_{+1}\text{Ti}^{4+}_{-2}$. Ve ferrocolumbitu jsou substituce opačné (a lokálně pravděpodobně kombinované s nepatrnným podílem kvantitativně nedefinovaných substitucí): $(\text{Fe},\text{Sc})^{3+}_{+3}(\text{Nb},\text{Ta})^{5+}_{+3}$, $(\text{Fe},\text{Mn},\text{Mg},\text{Ca})^{2+}_{-2}(\text{Nb},\text{Ta})^{5+}_{-4}$ a $(\text{Ti},\text{Zr},\text{Hf})^{4+}_{+3}(\text{Fe},\text{Mn},\text{Mg},\text{Ca})^{2+}_{-1}(\text{Nb},\text{Ta})^{5+}_{-2}$. Odmíšení vede k přednostní koncentraci Mg, Mn, Fe^{2+} , Fe^{3+} , Sc, Zr, Hf, U, Nb, Ta a W ve ferrocolumbitu. V relativním meřítku, rutil konservuje Sn, Fe^{2+} , Fe^{3+} , Ta a Fe^{3+} v poměru k Fe^{2+} , zatímco Mn a Nb jsou preferovány v columbitové struktuře. Obsah ZrO_2 v primárním homogenním niobovém rutilu je ≤ 0.34 hm. %, ale odmíšený ferrocolumbit obsahuje až 2.11 hm. % spolu s ≤ 0.16 hm. % HfO_2 . Tyto koncentrace potvrzují že Zr a Hf musejí být brány v potaz jako významné stopové prvky v niobovém rutilu z granitických asociací. Zvýšené obsahy MgO , ≤ 0.34 hm. % v primárním homogenním niobovém rutilu a ≤ 2.16 hm. % v odmíšeném ferrocolumbitu, jsou zřejmě lokálním zjevem, a nasvědčují kontaminaci serpentinitovou boční horninou.